Water Practice & Technology

IWA PUBLISHING

Water Practice & Technology Vol 18 No 11, 2957 doi: 10.2166/wpt.2023.196

Phosphorus removal from ore waste in aqueous solution with different mass of ore waste adsorbent from the Johor mine site

Noorul Hudai Abdullah [a,*], Wazif Hilmi Ahmad Nizam[a], Muhammad Habil Izzuddin Norhisham[a], Nur Audrizety Husaimi[a], Norhayati Ngadiman[a], Nur Atikah Abdul Salim[b], Norzainariah Abu Hassan[c] and Nur Husna Muslim[d]

[a] Neo Environmental Technology, Centre for Diploma Studies, Universiti Tun Hussein Onn Malaysia, Pagoh Education Hub, 84600 Pagoh, Johor, Malaysia
[b] School of Occupational, Safety & Health, Netherlands Maritime University College, Johor Bahru, Johor 80000, Malaysia
[c] Department of Civil Engineering, Politeknik Melaka, No. 2, Jalan PPM10, Plaza Pandan Malim, 75250 Melaka, Malaysia
[d] Faculty of Engineering Technology, Universiti Tun Hussein Onn Malaysia, Hab Pendidikan Tinggi Pagoh, Km 1, Jalan Panchor, 84600 Muar, Johor, Malaysia
*Corresponding author. E-mail: noorul@uthm.edu.my

NHA, 0000-0002-7303-6974

ABSTRACT

Mine waste management is becoming a growing global environmental concern for mining industries all over the world. Due to the abundance of ore waste from mining industries, this study aimed to observe the possibility of using ore waste to remove phosphorus from a solution. Although phosphorus is one of the essential elements for plant life, excessive phosphorus in water becomes one of the environmental issues, e.g., eutrophication. This study analysed the prediction contour of removal efficiency with the mass of adsorbent needed under different initial concentrations of solution. The batch experiment used an aqueous solution of 5 mg/L using potassium dihydrogen phosphate (KH_2PO_4) at different masses of adsorbent (2, 4, 6, 8, 10 g). The highest removal efficiency for phosphorus using 10 g of adsorbent is 54.3%. The data verified that the pseudo-second-order model (0.9976) fitted well. The adsorption between ore waste adsorbent and phosphorus was chemical sorption, whereas the analysis of isotherm models fitted the Freundlich model, with the occurrence of multilayer adsorption on the adsorption surface. The ability of ore waste to remove phosphorus was successful. This approach is one of the alternatives to enhance tertiary wastewater treatment technologies.

Key words: adsorbent, isotherm model, kinetic, ore waste, phosphorus, tertiary wastewater treatment

HIGHLIGHTS

- This study investigates the potential of phosphate removal onto ore waste adsorbent from the Johor mine site.
- The batch experiment used an aqueous solution of 5 mg/L using potassium dihydrogen phosphate at different masses of adsorbent (2, 4, 6, 8, and 10 g).
- The experimental data verified using kinetic and isotherm modelling studies supported with the physiochemical properties.

GRAPHICAL ABSTRACT

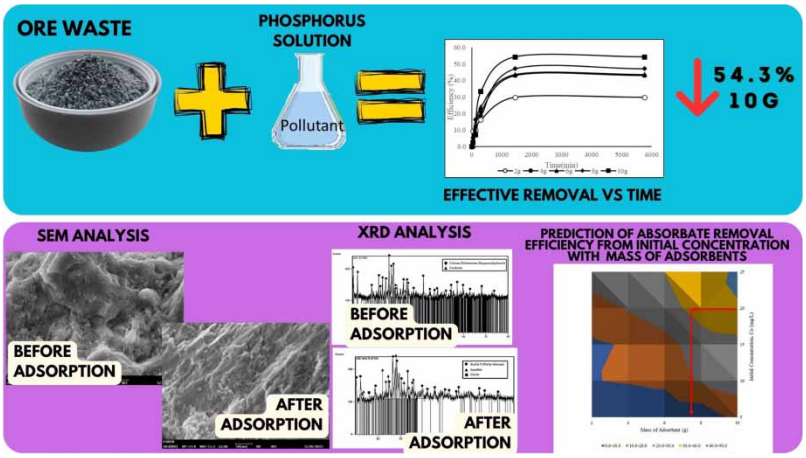

1. INTRODUCTION

The most significant environmental problem affecting lakes, reservoirs, rivers, and many other aquatic ecosystems is eutrophication, which is a reason for deteriorating water quality and severely limiting water usage (Preisner & Smol 2022). Eutrophication is caused by the excessive addition of nutrients, most notably phosphorus, to water bodies. When eutrophic circumstances occur, poisonous-reduced compounds increase, causing foul odours and tastes and hypolimnetic oxygen depletion (Nguyen *et al.* 2022). Eutrophication decreases the aquatic life population. An increase in nutrients (phosphorus) promotes the growth of aquatic plants and the formation of organic matter in the body of water, thus resulting in other aquatic life such as fish dying because of the high oxygen demand in the water body (Erhunmwunse *et al.* 2013). Phosphorus in domestic wastewater has been a big problem in big cities and also small villages (Chrispim *et al.* 2019). The main source of this pollution could be traced back to the household from soap, shampoo, and many other cleaning supplies that are used without a second thought and discharged away. Moreover, the excessive use of fertilizer in agriculture to provide nutrients for plants will cause the phosphorus pollutant to infiltrate into ground and surface water. It causes the beginning of the eutrophication process in the river due to uncontrolled human activities.

Phosphorus is one of the elements that can be removed through chemical or biological treatment at tertiary wastewater treatment. Due to the high maintenance and operational cost of phosphorus removal, this study approached the possibility of waste material, which is ore waste, to remove phosphorus in a solution (Martí *et al.* 2021). Ore waste is one of the products used as a train rock ballast in cement aggregate and asphalt aggregate. Other than that, ore waste does not have significant use over time, leading to an abundance of unused ore waste (Pashkevich & Petrova 2019). Despite its uselessness, ore waste contains elements that can contribute to removing phosphorus from the wastewater. One of the components, calcium dialuminium diaquaoctahydroxide 1.84-hydrate, has the ability to remove phosphorus from this wastewater and speed up the adsorption process (Nobaharan *et al.* 2021). Ore is also very cheap in the market, making it one of the most cost-efficient materials for removing phosphorus if the study is to be a definite success.

The possibility of ore waste in removing phosphorus from water is one of the novel causes that can be used in the adsorption treatment process. Although the adsorption of phosphorus is practically used various materials in previous studies, this study focuses on analysis to verify the theoretical and experimental data. The mathematical models apply the adsorption of solute through surface porous adsorbent, mass of adsorption, and initial concentration to develop the prediction on removing pollutants in water (Chung *et al.* 2015). The use of kinetic and isotherm models as well as a prediction on removal efficiency through different initial concentrations and required mass of adsorbent still need to be investigated due to ore waste, one of the novel adsorbents in the water treatment process. The objectives of this study are (1) to investigate the removal performance of ore waste in removing phosphorus from synthetic wastewater, (2) to verify the theoretical and batch experimental data using kinetic (pseudo-first-order (PFO) and pseudo-second-order (PSO)) and isotherm (Langmuir and kinetic) modelling studies, and (3) to create the prediction contour of removal efficiency and the mass of adsorbent needed under the different initial concentrations of phosphorus solution.

2. METHODS

2.1. Preparation of adsorbent

Adsorbent was prepared by first collecting 1 kg of ore waste at the Johor mine site. The ore waste was then sun-dried for 2 days. In order to obtain complete drying, the dried ore waste was dried again in a drying oven at 30 °C for 2 days. The dry absorbent was then sieved to achieve a size range of 1.18–2.46 mm and weighed using an analytical balance for 2, 4, 6, 8, and 10 g for batch experiments.

2.2. Preparation of synthetic solutions

In a volumetric flask, 0.1433 g of potassium dihydrogen phosphate (KH_2PO_4) was dissolved in 1 L of deionised water to make 100 mg/L PO_4^{3-} solution. The solution was then diluted to 5, 10, 15, 20, and 25 mg/L PO_4^{3-} concentrations.

2.3. Analytical methods

The amino acid method 8178 programmed was used to assess the initial and final phosphorus concentrations in aqueous solutions using the HACH DR 6000 UV-VIS Spectrophotometer. The researchers employed the COXEM EM – 30 AXE PLUS SEM to assess SEM testing for surface morphology of the membrane and EDXRF for identify the chemical elements group on the ore waste. The Perkin Elmer Spectrum Two FTIR Spectrometer was used to characterise the functional groups of the ore and display the infrared adsorption spectrum before and after the adsorption process. The researchers employed a second-generation BRUKER D2 Phaser Benchtop XRD to analyse the crystallisation or crystal-phase composition of the shell in XRD analysis.

2.4. Preparation of synthetic solutions

Two batch experiments were carried out for the adsorption study using an aqueous solution. The first batch experiment investigated the initial concentration and adsorbent mass effects by introducing 2, 4, 6, 8, and 10 g of adsorbent into a conical flask of 100 mL with varying concentrations. Each conical flask was mixed with a synthetic solution with 5, 10, 15, 20, and 25 phosphorus concentrations for 5,760 min and shaken at 170 rpm.

A series of second-batch tests explore the influence of absorbent mass and time. The influence of adsorbent mass was investigated in the second group using 2, 4, 6, 8, and 10 g of absorbent in a 100 mL conical flask with varying contact lengths of 30, 120, 300, 1,440, and 5,760 min and shaken in 170 rpm. After filtering each sample with a filtration pump to separate the solution from the suspended particles, the phosphate content was analysed using the DR6000 UV-Spectrophotometer, and the data were verified through kinetic and isotherm models.

2.5. Adsorption kinetic models

2.5.1. PFO kinetic model

The key idea behind the PFO kinetic model is the total rate of unoccupied sites corresponding to occupied sorption sites. Many models for diverse solute adsorption have been developed, but it is still important to evaluate the applicability and consistency of both their linear and nonlinear forms (Kajjumba *et al.* 2018). The PFO equation is typically written in the following equation:

$$\ln(q_e - q_t) = \ln(q_e) - k_1 - t_i \tag{1}$$

where q_t (mg/g) and q_e (mg/g) denote the concentrations of solute adsorbed and adsorbent at any given time and equilibrium, respectively, and k_1 is the PFO model rate constant (Revellame *et al.* 2020).

2.5.2. PSO kinetic model

The PSO kinetic model assumes that the total amount of solute adsorbed equals the number of accessible sites on the adsorbent. Furthermore, the number of active sites equals the kinetics, and the response rate is proportional to the solute concentration on the adsorbent's surface. This model is expressed in the following equation:

$$\frac{t_i}{q_t} = \frac{1}{k_2 q_e^2} + \frac{t_i}{q_e} \tag{2}$$

where q_t (mg/g) represents the concentration of phosphorus adsorbed at any time t, q_e (mg/g) represents the concentration of adsorbed phosphorus at equilibrium, and k_2 represents the PSO constant, which may be found by graphing t/q against t_i (Debnath & Das 2023).

2.6. Adsorption isotherm models

The adsorption isotherm is critical in identifying the adsorbent and the adsorbent response. This process will provide adequate evidence that an efficient adsorbent may be absorbed. The form of the isotherm expresses both the durability of the adsorbent–adsorbate interactions and the adsorption affinities of the molecules.

2.6.1. Langmuir isotherm

When the adsorption process reaches equilibrium, the isotherm gives the most critical information by displaying how the adsorbate molecules are distributed uniformly across the liquid and solid phases (Farro *et al.* 2023). The Langmuir isotherm is expressed in a linear form in the following equation:

$$\frac{1}{q_e} = \frac{1}{K_L q_{\max} C_e} + \frac{1}{q_{\max}} \tag{3}$$

where q_e is the equilibrium adsorption capacity in mg/g and C_e is the metal equilibrium concentration in solution (mg/L). The maximum sorption capacity, $q_{\max}$, should be temperature-dependent, indicating that the sorbate is covered by a single layer of sorption, and the enthalpy of sorption, K_L (Li *et al.* 2021).

2.6.2. Freundlich isotherm

The Freundlich sorption isotherm is a famous mathematical model because it can account for various concentrations and is widely utilised in practice. This isotherm showed how different the surface was and how the number of active sites and energy increased exponentially (Li *et al.* 2021). The linear Freundlich isotherm model is expressed in the following equation:

$$\ln\ q_e = \ln K_f + \frac{1}{n} \ln (C_e) \tag{4}$$

where q_e is the equilibrium amount of metal ion adsorbed per gram of adsorbent (mg/g), C_e is the equilibrium concentration of metal ions in the solution (mg/L), and K_f and $1/n$ are the Freundlich model constants. The result of plotting $\ln q_e$ versus $\ln(C_e)$ is a linear relationship with the slope equal to $1/n$ and the intercept equal to $\ln K_f$ (Li *et al.* 2021).

3. RESULTS AND DISCUSSION

3.1. Physicochemical characteristics of adsorbent

3.1.1. SEM and EDXRF analyses

Analysis using EDXRF and SEM revealed the characterisation of discarded raw ore. The surface morphology of the ore waste is depicted in Figure 1 at a magnification of 2,000 and 5,000 times for before (Figure 1(a) and 1(b)) and after (Figure 1(c) and 1(d)), and adsorption of phosphorus in solution. Figure 1(a) and 1(b) depicts a surface morphology view of a thick, uneven, rocky, and seemingly impermeable raw ore waste. Figure 1(c) and 1(d) depict a surface morphology of raw ore waste that is still compact, rocky, and more organised than before adsorption and yet seems to be completely without porosity. Due to the reaction between the ore and phosphorus in Figure 1(c) and 1(d), the ore has been somewhat eroded and has become more organised than before adsorption.

EDXRF was used to evaluate the elemental compositions of mining waste. Table 1 lists the elements that make up ore waste. Before the reaction between the ore waste and phosphorus, the major elements in the ore waste were Si and O, with measurements of 26.22 and 52.38%, respectively. In contrast, the major elements in the ore waste of the reaction with phosphorus afterwards were Si and Ca, with measurements of 48.40 and 24.79%, respectively. It is also shown that O was not in the ore waste anymore after the reaction with the phosphorus. Elements with calcium often have the ability to remove phosphorus from the aqueous solution (Nguyen *et al.* 2022). This means it is confirmed that ore waste can potentially remove phosphorus from wastewater. Table 1 also shows that after the reaction between the ore and phosphorus, there is an increase in the percentage of the elemental composition in the ore.

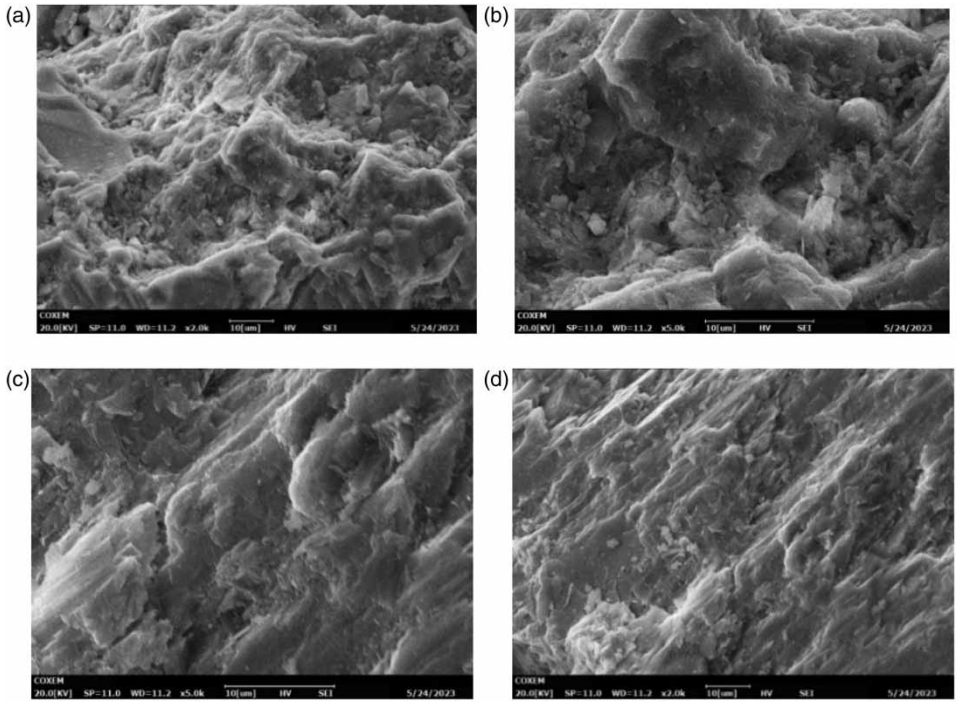

Figure 1 | SEM photomicrograph for raw ore waste: (a) 2,000× and (b) 5,000× magnification for before adsorption; (c) 2,000× and (d) 5,000× magnification for after adsorption.

Table 1 | Percentage of elemental compositions of the raw ore waste sample

Elemental compositions	Before (%)	After (%)
Si	26.22	48.40
Ca	5.99	24.79
Al	10.94	21.49
Na	4.38	4.78
P	0.06	0.55
O	52.38	0.00
Total	100.00	100.00

3.1.2. XRD analysis

The purity and crystallinity of inorganic 'materials' are determined by x-ray diffraction (XRD) (Zhao *et al*. 2022). In order to discover more about the ore waste complex before and after phosphate absorption, an XRD pattern analysis was employed. Figure 2(a) represents the ore waste before phosphorus absorption, revealing four

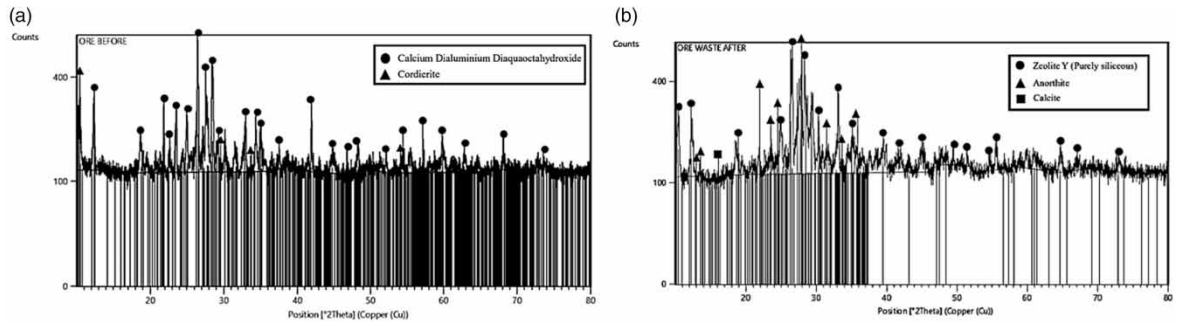

Figure 2 | XRD pattern of ore waste (a) before and (b) after phosphorus adsorption from the aqueous solution.

elements, including calcium dialuminium diaquaoctahydroxide, cordierite, aerinite, and sodium potassium hydride. The triangle represents cordierite, whereas the line with the circle symbol represents calcium dialuminium diaquaoctahydroxide. Since ion exchange is possible, trace elements such as Ca^{2+} and Al^{3+} ions are present in calcium dialuminium diaquaoctahydroxide. Ore waste has a good absorption capacity for eliminating PO_4^{3-} from water (Li *et al.* 2021).

The cordierite line with a triangle symbol is the substance with the second-highest dominating peak visible in the XRD pattern in Figure 2(a). A magnesium–iron aluminium cyclosilicate, cordierite is sometimes called dichroite and iolite (Guo *et al.* 2022). Because phosphate is a cation, the presence of positive ions such as Mg^{2+} and Al^{3+} might enhance the adsorption of phosphate. Since cordierite is currently employed extensively in the electronic and information fields thanks to its superior electrical, thermal, and mechanical qualities, ore waste can now be used more broadly for purposes other than only water treatment (Othman *et al.* 2021).

The prominent peak in the XRD pattern in Figure 2(b) is the line with the circle symbol. The triangle and square symbols represent the second and third dominating peaks. The triangle and square symbols represent anorthite and calcite, respectively, whereas the circle represents zeolite Y (purely siliceous). Crystalline-hydrated aluminium silicates make up zeolite. The hydrated zeolites display a consistent three-dimensional crystalline aluminosilicate structure based on tetrahedrons, where silicon or aluminium cations are surrounded by four oxygen atoms at the vertices, signifying $(SiO_4)^{4-}$ and $(AlO_4)^{5-}$ (Farro *et al.* 2023). Any zeolite is highly microporous because these structures create a network of pores and channels. Depending on the width of the pores, any zeolite can adsorb water and cations (Pashkevich & Petrova 2019). As a result, zeolite-containing ore waste can be used to remove phosphate from water.

Calcium silicate has recently emerged as an adsorptive material with tremendous potential for phosphate removal from other adsorbents. Calcium silicate can be used for phosphate recovery in biological wastewater treatment because it acts as a calcium ion donor under low supersaturation and alkaline conditions (pH = 8–9). Anorthite that contains calcium silicate can promote the nucleation process as a crystal seed, which is easier to precipitate and recover than the conventional calcium phosphate compound (Guo *et al.* 2022).

Calcite has been shown in studies to eliminate phosphate successfully. Extensive studies on phosphate adsorption by calcite have been done at low phosphate concentrations (Li *et al.* 2021). Langmuir adsorption isotherms can be used to describe phosphate adsorption by calcite, which is most likely due to monolayer adsorption. According to research, over 80% of phosphate anions were adsorbed within 10 s, probably because phosphate ions replaced adsorbed water molecules, bicarbonate ions, or hydroxyl ions from calcite surfaces.

3.1.3. FTIR analysis

Fourier transform infra-red analysis can be used to identify the chemical composition of the sample and to determine the presence of specific functional groups or chemical bonds (Agatonovic-Kustrin *et al.* 2021). FTIR machines are commonly used in various fields, including chemistry, materials science, and biology, to analyse samples ranging from small molecules to complex biological systems (Farro *et al.* 2023). The samples are run before and after the reaction with phosphorus, as shown in Figure 3.

The frequencies of the ore waste sample before the adsorption process were 658.447, 756.514, and 940.118 cm^{-1}. The frequencies significantly change after the reaction with aqueous phosphorus solution to 687.640, 755.900, and 946.297 cm^{-1}. The difference between the frequencies of 29.193 cm^{-1} (658.447–687.640 cm^{-1}) was attributed to C–Cl stretching (Cao *et al.* 2022). The adsorption of phosphorus changes the frequency of C–H bending to 0.61 4 cm^{-1} (756.514–755.900 cm^{-1}). The reaction between the ore waste and the phosphorus solution caused the frequency of C–C bending to change from 940.118 to 946.297 cm^{-1}, with the differences of −6.179 cm^{-1} in frequency (Possenti *et al.* 2021; Sambuu 2021). As we can see from Table 2, there are other frequencies that do not have any changes or appeared after the reaction such as the frequency of 1,216.910 cm^{-1} associated with C–O stretching (Abdullah *et al.* 2023). Another one is at frequency 1,372.840 cm^{-1}, which is in the functional group of S = O stretching. Next on the table is frequency 1,434.395 cm^{-1}, which is detected in group of O–H bending (Li *et al.* 2022). After that, the frequency of 1,738.286 cm^{-1} is associated with the functional group of C = C = C stretching (Giachet *et al.* 2021; Hien *et al.* 2022). After the reaction of ore waste and phosphorus, there is appearance of the frequency of 1,954.640 cm^{-1}, which is detected in the functional group of C = O stretching, and the last one is the frequency of 3,019.126 cm^{-1}, which is in the functional group of C–H stretching (Metlenkin *et al.* 2022).

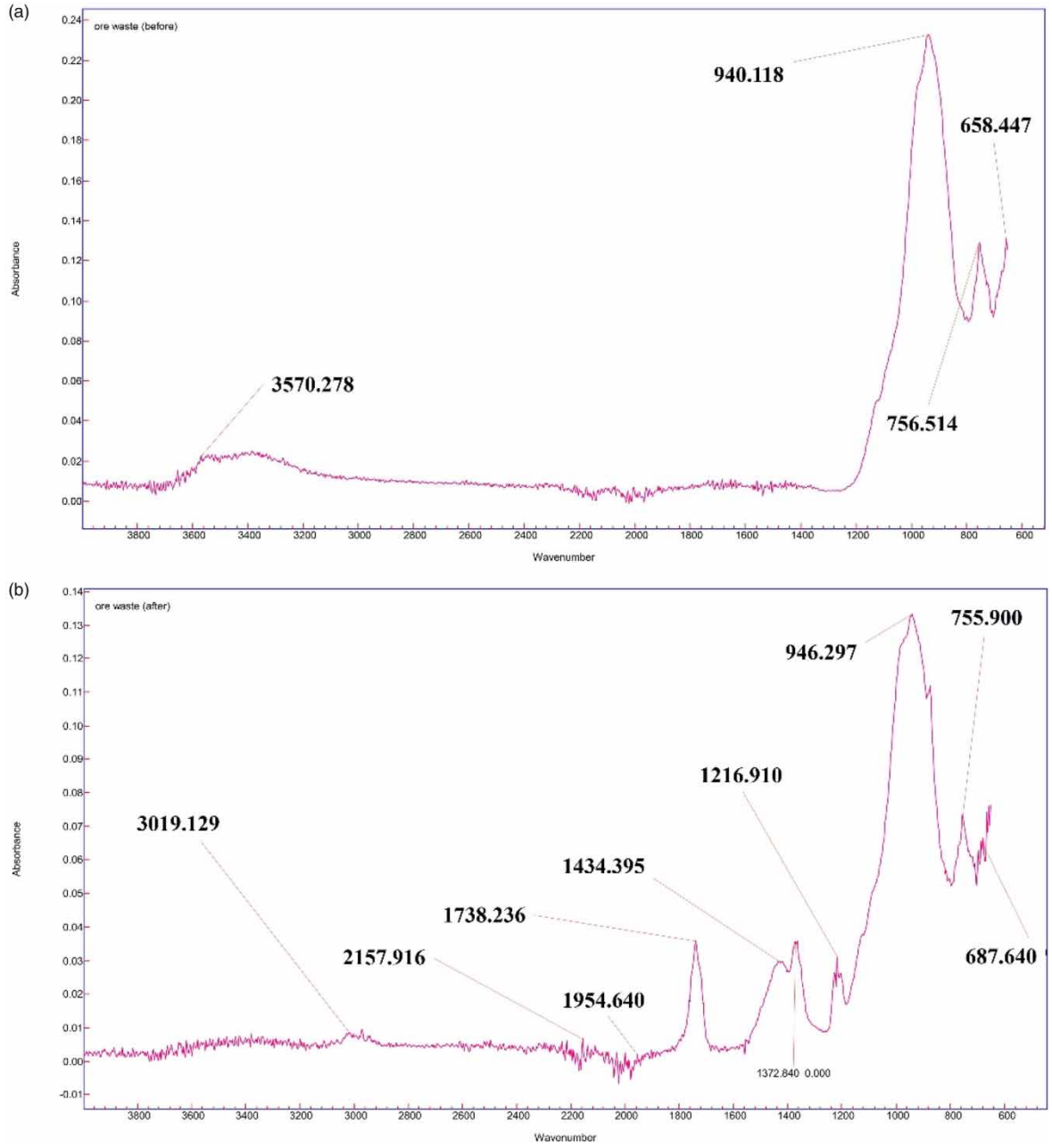

Figure 3 | FTIR analysis on ore waste: (a) before and (b) after adsorption.

3.2. Adsorption of phosphorus onto ore waste

The rate of phosphorus adsorption on ore waste was tracked over time to estimate the equilibrium-corresponding contact period. This was carried out so that the link between monitoring adsorption uptake over time at a particular pressure or concentration can be observed in adsorption kinetics, which is used to quantify the quantity of diffusion adsorbate that contacts pores (Debnath & Das 2023). Due to the active surface sites present at the start of the adsorption and those that remain after a certain period, the first few minutes may be defined as the speed of adsorption kinetic presence in a substantial quantity, as adsorption is the transition from liquid to solid phase (Martí *et al.* 2021).

Adsorption capacity performance is defined as the quantity of adsorbate adsorbed per unit mass (Liu & Guo 2022). Adsorption ability refers to the total value of the ore waste used in this study to adsorb phosphorus from wastewater or the adsorption potential of each particle mass. The following equation was used to compute the

Table 2 | FTIR spectrum of ore waste before and after the adsorption of phosphorus

Before adsorption	After adsorption	Differences	Detection of functional group	References
658.447	687.640	−29.193	C–Cl stretching	Agatonovic-Kustrin *et al.* (2021)
756.514	755.900	0.614	C–H bending	
940.118	946.297	−6.179	C–C bending	
3,570.278	–	–	O–H stretching	
–	1,216.910	–	C–O stretching	Phawachalotorn *et al.* (2023)
–	1,372.840	–	S = O stretching	
–	1,434.395	–	O–H bending	
–	1,738.286	–	C = C = C stretching	Abdullah *et al.* (2023)
–	1,954.640	–	C = O stretching	
–	3,019.126	–	C–H stretching	

adsorption capacity in the following equation:

$$q = \frac{C_i - C_f}{m} \times V \tag{5}$$

In the equation, q is the amount of phosphorus that has been adsorbed at equilibrium (mg/g), C_i is the starting phosphorus concentration (mg/L), C_f is the equilibrium phosphorus concentration (mg/L), V is the solution volume (L), and m is the ore mass (g) in the solution. Figure 4 depicts the adsorption capacity from the start of the experiment to equilibrium using the formula for each particle mass.

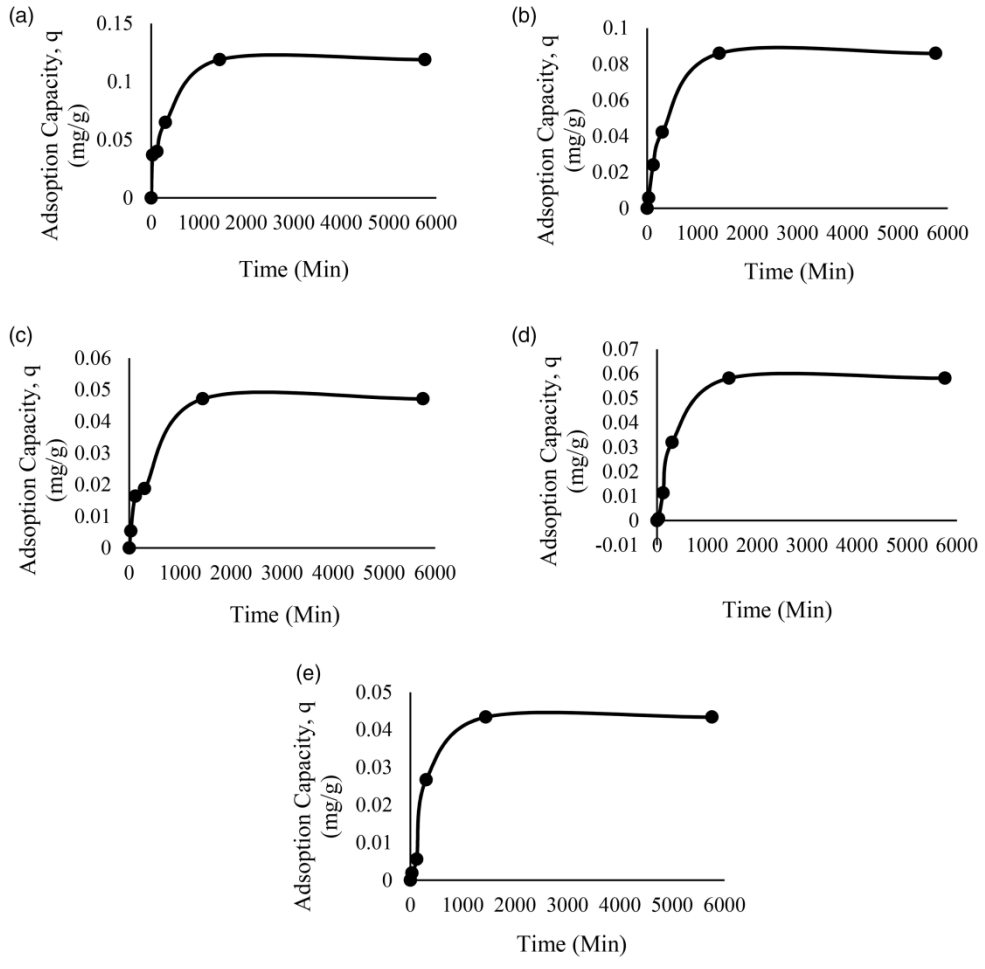

Figure 4 | Effect of adsorption capacity on phosphate removal: (a) 2 g, (b) 4 g, (c) 6 g, (d) 8 g, and (e)10 g.

Figure 4 shows the adsorption capacity performance for five different particle masses of mining waste. The adsorption capacity for each particle mass achieved equilibrium at 1,440 min, and the adsorption capacity remained constant for the following 4,320 min. For each particle mass, the adsorption capacity, q_e, was 0.119 mg/g (2 g), 0.0860 mg/g (4 g), 0.0582 mg/g (6 g), 0.0471 mg/g (8 g), and 0.0434 mg/g (10 g).

The adsorbent's removal efficiency was also measured to assess how well ore waste adsorbs phosphorus from synthetic wastewater (Debnath & Das 2023). The following equation was used to calculate the removal efficiency E (%).

$$E = \frac{C_i - C_f}{v} \times 100\% \tag{6}$$

Figure 5(a) depicts the performance of removal efficiency against contact time. As the contact duration rises, the removal efficiency increases fast, demonstrating the rapid process of adsorbate filling the unoccupied sites on the porous surface of the adsorbent until equilibrium was reached when all the vacant sites were entirely occupied. For each particle mass, the greatest removal effectiveness was 29.8% (2 g), 43.0% (4 g), 43.6% (6 g), 47.1% (8 g), and 54.3% (10 g). The greatest removal efficiency and q_e relationship were plotted versus particle mass. The trend demonstrates that when the removal efficiency improves, the adsorption capacity decreases, indicating that the adsorption process at active sites becomes faster, as illustrated in Figure 5(b).

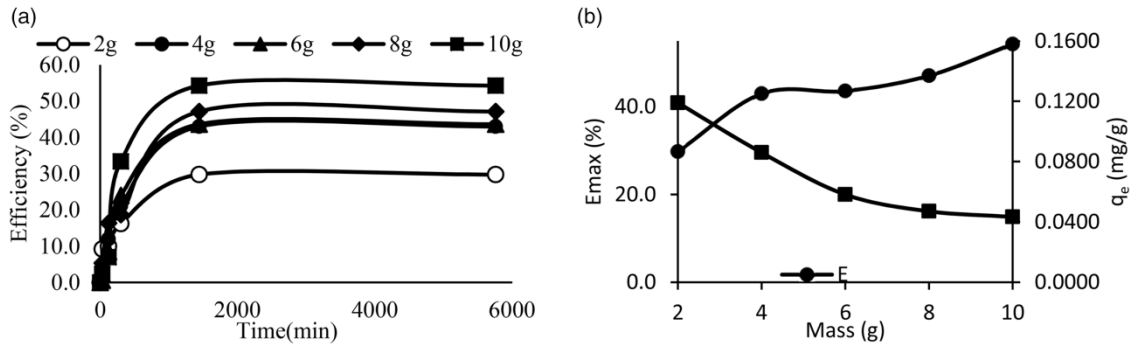

Figure 5 | (a) The performance of removal efficiency, E (%) against time, t (min) for every particle mass. (b) Effect of the different masses of the adsorbent on the adsorption capacity, q_e and E.

3.3. Adsorption kinetic model

The adsorption process was examined using the PFO and PSO kinetic models. The F_e and R^2 values for both models were calculated, and the models were compared to determine which model best represents the adsorption kinetic with the greatest R^2 and lowest F_e (Pashkevich & Petrova 2019). F_e was computed using Equation (7).

$$F_e = \sqrt{\left(\frac{1}{n-p}\right) \sum_{i}^{n} \left(q_{t(\exp)} - q_{t(\text{theo})}\right)} \tag{7}$$

where n represents the number of measurements, p is the number of kinetic parameters, and $q_{t(\exp)}$ and $q_{t(theo)}$ are the experimental and theoretical adsorption capacities, respectively. As seen in Figure 6(a), the graph was produced by fitting the data into the PFO model.

Table 3 demonstrates that the particle mass 10 g has an excellent adsorption capacity and removal efficiency, with the highest R^2 (0.5242) and a low F_e (1.2215). In contrast, the particle mass 8 g has poor adsorption capacity but a good removal efficiency, with the lowest R^2value (0.3885) and the lowest F_e value (0.9870) for PFO analysis.

The PFO kinetic model, which assumes that chemical sorption or chemisorption is the rate-limiting phase, predicts the behaviour across the whole adsorption range. In this case, adsorption capacity, not adsorbate concentration, dictates the adsorption rate. Figure 6(b) depicts the linear regression analysis for the PSO kinetic model. Table 3 indicates that all particle masses have an excellent coefficient correlation that is close to 1 for PSO analysis. However, particle mass 2 g has the greatest R^2 value (0.9976) of all particle masses, indicating that it has

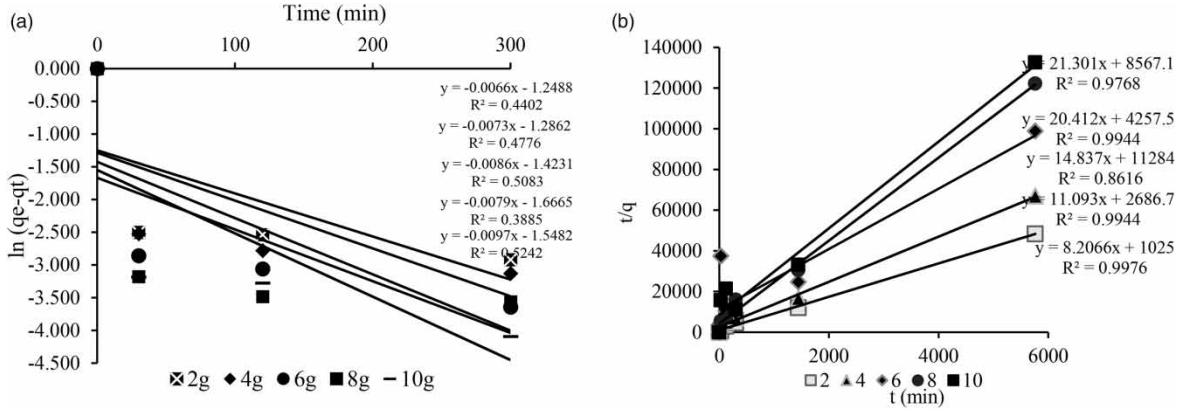

Figure 6 | (a) Linear regression analysis for the PFO model on the adsorption of PO_4^{3-} onto adsorbent from an aqueous solution. (b) PSO model for the adsorption of PO_4^{3-} onto adsorbent from an aqueous solution.

Table 3 | Kinetic parameter of PFO and PSO model parameters

Kinetic parameter of the PFO model

Mass of adsorbent (g)	$q_{e(theo)}$ (mg/g)	K_1 (min^{-1})	R^2	F_e	$q_{e(exp)}$ (mg/g)
2	0.2868	0.0066	0.4402	1.1247	0.1190
4	0.2763	0.0071	0.4776	1.3330	0.0860
6	0.2410	0.0086	0.5083	1.3060	0.0582
8	0.1889	0.0079	0.3885	0.9870	0.0471
10	0.2126	0.0097	0.5242	1.2215	0.0434

Kinetic parameter of the PSO model

Mass of adsorbent (g)	$q_{e(theo)}$ (mg/g)	K_2 (min^{-1})	R^2	F_e	$q_{e(exp)}$ (mg/g)
2	0.1219	0.0657	0.9976	0.0433	0.1190
4	0.0901	0.0458	0.9944	0.0190	0.0860
6	0.0674	0.0195	0.8616	0.0228	0.0582
8	0.0490	0.0979	0.9944	0.0119	0.0471
10	0.0469	0.0530	0.9768	0.0097	0.0434

the highest adsorption rate. It proves that ore waste reacts better to phosphorus through chemical than physical reactions.

It has been concluded that the PSO model is the better kinetic model to reflect adsorption kinetics since it has the highest R^2 value (0.9976) compared to the PFO model (0.5242). Furthermore, the value of F_e of the PSO model (0.0097) is smaller than that of the PFO model (0.9870). This demonstrates that the data fit better with the PSO model than the PFO model. In addition, the best fit demonstrates that the adsorption process depends on the adsorbate and adsorbent quantities (Debnath & Das 2023). Once again, the value of R^2 shows that the results support the intra-particle diffusion hypothesis, which sheds light on the adsorption mechanism. The adsorption process is better represented by PSO kinetics if the PSO rate constant is greater than the PFO rate constant. This would imply that rather than only the surface reaction, the adsorption process is predominantly governed by both surface reaction and diffusion (Kalam *et al.* 2021).

3.4. Adsorption isotherm model

The adsorption mechanism is commonly explicated by applying isotherms, which are mathematical functions that establish a relationship between the quantities of the adsorbate present on the adsorbent material. Various isotherm models, including Langmuir and Freundlich, can characterise the partitioning of metal ions between the liquid and solid phases. The Langmuir isotherm model postulates that adsorption occurs in a single layer on a

surface with a limited number of adsorption sites with uniform characteristics and that the adsorbate has no lateral movement on the surface. Once a site has reached its maximum sorption capacity, it can no longer undergo additional sorption processes. This means that the surface attains a state of saturation wherein the highest level of adsorption possible for the surface is attained.

The Freundlich isotherm model is based on the simultaneous adsorption of cation and anion on the same adsorbent surface. The Freundlich isotherm model, based on multilayer adsorption, is used to define adsorption processes that occur on heterogeneous surfaces and active sites (Liu & Guo 2022). When the data were fitted into the model, the linear plot of the Freundlich model was obtained, as shown in Figure 7(a). The R^2 value is 0.8418 for the Freundlich model, which is more than that of the Langmuir model (Figure 7(b)), indicating that it is a better adsorption isotherm model for this study.

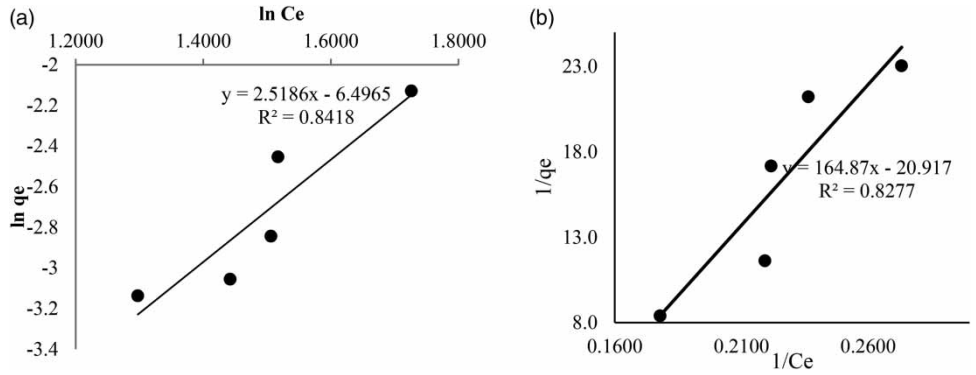

Figure 7 | Linear plot of (a) Freundlich model of ln(C_e) against ln q_e and (b) Langmuir model of 1/C_e against 1/q_e for the adsorption of PO_4^{3-} onto adsorbent from the synthetic solution.

The results indicate that ore residue can absorb PO_4^{3-} from the synthetic solution. This ability is because calcium oxide on the surfaces of raw ore waste and phosphate ions has a strong affinity for one another due to their distinct charges. Table 1 displaying EDXRF analysis shows that ore waste can remove phosphorus from wastewater because materials containing Ca can remove phosphorus from the aqueous solution. The calcination process alters the physical and chemical properties of calcium carbonate and ore residues (Preisner & Smol 2022).

Linear plots were obtained in both cases, indicating the suitability of these isotherms for the current adsorption process. The present study showcases the Langmuir and Freundlich plots of figures and exhibits the adsorption of calcium onto ore waste. Table 4 enumerates the distinct Langmuir and Freundlich constants derived from these plots.

Table 4 | Freundlich and Langmuir of the isotherm model parameters

Freundlich model			Langmuir model		
n	K_F (mg/g)	R^2	q_{max} (mg/g)	K_L (mg/g)	R^2
0.3970	0.0015	0.8418	−0.0478	−0.12689	0.8277

Table 4 presents the Langmuir and Freundlich adsorption constants and the correlation coefficients denoted by R^2. In order to determine the optimal model for the adsorption of calcium, the data were subjected to fitting using the Langmuir and Freundlich isotherm models. The results indicate satisfactory conformity with the Freundlich model ($R^2 = 0.8418$) in contrast to the utilisation of the Langmuir isotherm model ($R^2 = 0.827$). The Freundlich equation yielded a n-value of 0.3970, as presented in Table 4. This suggests that the utilisation of ore waste involves a chemical process.

3.5. Prediction of adsorbate removal efficiency or required mass adsorbent

The study conducted several batches of experiments to investigate the efficacy of ore waste in removing phosphorus compounds from aqueous solutions and creating contour prediction, as shown in Figure 8 (Chung *et al.* 2015). The findings of this experiment based on the batch study demonstrated that the removal efficiencies are directly proportional to the weight of the sample being analysed. According to Figure 8, the quantity of phosphorus that can be removed from an aqueous solution with an initial concentration of 20 mg/L using 7.5 g of ore waste ranges from 40 to 30% (Point A). In contrast, the amount of 5.2 g of ore waste can remove 10–20% phosphorus from an aqueous solution containing 12.5 mg/L initial concentration. Furthermore, 3.5 g of ore waste can remove phosphorus from the solution as much as 10–20% using a 15 mg/L initial concentration (Point C).

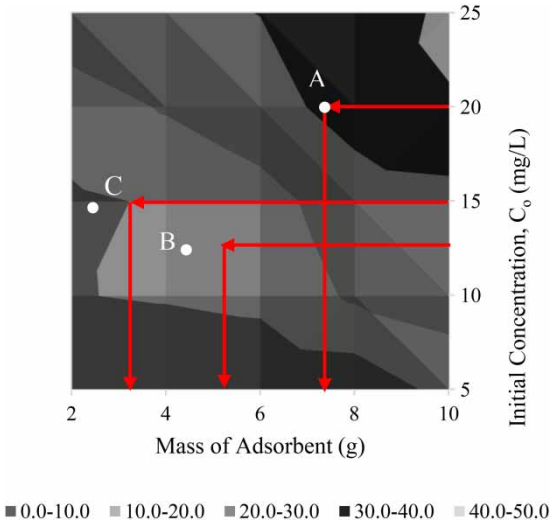

Figure 8 | Contour diagram of removal efficiency on the removal of phosphate using ore waste.

Even though more precise values could be calculated by explicitly applying the developed equations, plots similar to those in Figure 8 would be useful for quickly determining the removal efficiency trend as a function of the initial adsorption conditions. Such plots enable a clearer understanding of the relationship between removal efficiency and initial adsorption conditions.

4. CONCLUSIONS

The present work evaluated the removal performance of phosphate using ore waste and showed that this natural adsorbent could be considered an efficient material for phosphorus removal from wastewater. Ore waste, mainly composed of calcium, is a potential material for wastewater treatment since precipitation with carbonate is commonly employed for phosphate removal from wastewater. Based on the batch test experiments, all parameters significantly impact phosphate removal efficiency, and mass adsorbent has proved to be the key variable in this study. Experiment results showed that when mass adsorbent increased, phosphate removal percentage also increased due to the increase in the surface area of the adsorbent particles. When the adsorbent dosage increased, the removal of metal ions increased, stimulating a greater phosphate removal process from the aqueous solution. The objectives of this study were achieved. Ore waste can remove phosphate in wastewater because it is rich in calcium. These findings demonstrated the successful removal of ore waste of up to 54.3% from the aqueous solution. The results indicate that the PSO kinetic model is well described with the absorption kinetic of phosphate onto ore waste due to the higher value of R^2, which is 0.9976. It proves that ore waste reacts better to phosphorus through chemical reactions than through physical reactions. On the other hand, the Freundlich model was considered a more versatile system due to a greater degree of heterogeneity in the surface of absorbent material. Therefore, it can be concluded that more waste could be used because of its effectiveness as a natural adsorbent, which is easily accessible and economical. Ore waste can reduce the cost of treating wastewater, especially in removing phosphate, and promote an environmental-friendly solution of obtaining a cleaner water source.

ACKNOWLEDGEMENTS

This research was funded by Tier 1 Grant Vot Q407 and GPPS Grant Q317 provided by the Universiti Tun Hussein Onn Malaysia (UTHM). The authors would like to thank the Neo Environment Technology (NET), Centre for Diploma Studies (CeDS), Research Management Centre, UTHM, for their support.

DATA AVAILABILITY STATEMENT

All relevant data are included in the paper or its Supplementary Information.

CONFLICT OF INTEREST

The authors declare there is no conflict.

REFERENCES

Abdullah, N. H., Xian, O. J., Yi, C. Z., Yuan, N. S., Yaacob, M. S. S., Salim, N. A. A. & Abdullah, F. 2023 Removal of phosphate from synthetic wastewater by using marsh clam (*Polymesoda expansa*) shell as an adsorbent. *Biointerface Research in Applied Chemistry* **13**(1), 56.

Agatonovic-Kustrin, S., Gegechkori, V., Petrovich, D. S., Ilinichna, K. T. & Morton, D. W. 2021 HPTLC and FTIR fingerprinting of olive leaves extracts and ATR-FTIR characterisation of major flavonoids and polyphenolics. *Molecules* **26**(22), 6892.

Cao, C., Yang, J., Zeng, F., Liu, F., Yang, S. & Wang, Y. 2022 Morphology and FTIR characteristics of the alluvial diamond from the Yangtze Craton, China. *Crystals* **12**(4), 539.

Chrispim, M. C., Scholz, M. & Nolasco, M. A. 2019 Phosphorus recovery from municipal wastewater treatment: Critical review of challenges and opportunities for developing countries. *Journal of Environmental Management* **248**, 109268.

Chung, H. K., Kim, W. H., Park, J., Cho, J., Jeong, T. Y. & Park, P. K. 2015 Application of Langmuir and Freundlich isotherms to predict adsorbate removal efficiency or required amount of adsorbent. *Journal of Industrial and Engineering Chemistry* **28**, 241–246.

Debnath, S. & Das, R. 2023 Strong adsorption of CV dye by Ni ferrite nanoparticles for waste water purification: Fits well the pseudo second order kinetic and Freundlich isotherm model. *Ceramics International* **49**(2), 16199–16215.

Erhunmwunse, N. O., Dirisu, A. R. & Ogbeibu, A. E. 2013 Managing eutrophication in Nigeria inland waters. *Journal of Water Resource and Protection* **5**(07), 743.

Farro, N. W., Reyes, W., Mendoza, J. L., Veleva, L., Quintana, P., Azamar, J. A. & Aguilar, D. 2023 Characterization by XRD and FTIR of zeolite A and zeolite X obtained from fly ash. *Chemical Engineering Transactions* **99**, 679–684.

Giachet, M. T., Schröter, J. & Brambilla, L. 2021 Characterisation and identification of varnishes on copper alloys by means of UV imaging and FTIR. *Coatings* **11**(3), 11030298.

Guo, Z., Li, K., Jiang, L., Ran, Y., Sarkodie, E. K., Yang, J. & Liu, X. 2022 Removal mechanisms of phosphate from water by calcium silicate hydrate supported on hydrochar derived from microwave-assisted hydrothermal treatment. *Environmental Technology & Innovation* **28**, 102942.

Hien, L. T. T., Gobin, A., Lim, D. T., Quan, D. T., Hue, N. T., Thang, N. N. & Linh, P. H. 2022 Soil moisture influence on the FTIR spectrum of salt-affected soils. *Remote Sensing* **14**(10), 2380.

Kajjumba, G. W., Emik, S., Öngen, A., Özcan, H. K. & Aydın, S. 2018 Modelling of adsorption kinetic processes – Errors, theory and application. *Advanced Sorption Process Applications*, 1–19.

Kalam, S., Abu-Khamsin, S. A., Kamal, M. S. & Patil, S. 2021 Surfactant adsorption isotherms: A review. *ACS Omega* **6**(48), 32342–32348.

Li, Y., Nan, X., Li, D., Wang, L., Xu, R. & Li, Q. 2021 Advances in the treatment of phosphorus-containing wastewater. *IOP Conference Series: Earth and Environmental Science.* **647**(1), 012163.

Li, X., Zhao, X., Zhang, J., Hao, J. & Zhang, Q. 2022 Struvite crystallization by using active serpentine: An innovative application for the economical and efficient recovery of phosphorus from black water. *Water Research* **221**, 118678.

Liu, X. & Guo, Y. 2022 Study on the color-influencing factors of blue iolite. *Minerals* **12**(11), 1356.

Martí, V., Jubany, I., Ribas, D., Benito, J. A. & Ferrer, B. 2021 Improvement of phosphate adsorption kinetics onto ferric hydroxide by size reduction. *Water* **13**(11), 1558.

Metlenkin, D. A., Kiselev, N. V., Platov, Y. T., Khaidarov, B. B., Khaidarov, T. B., Kolesnikov, E. A. & Burmistrov, I. N. 2022 Identification of the elemental composition of granulated blast furnace slag by FTIR-spectroscopy and chemometrics. *Processes* **10**(11), 2166.

Nguyen, T. A. H., Le, T. V., Ngo, H. H., Guo, W. S., Vu, N. D., Tran, T. T. T. & Pham, T. T. 2022 Hybrid use of coal slag and calcined ferralsol as wetland substrate for improving phosphorus removal from wastewater. *Chemical Engineering Journal* **428**, 132124.

Nobaharan, K., Bagheri Novair, S., Asgari Lajayer, B. & van Hullebusch, E. D. 2021 Phosphorus removal from wastewater: The potential use of biochar and the key controlling factors. *Water* **13**(4), 517.

Othman, N. H., Alias, N. H., Fuzil, N. S., Marpani, F., Shahruddin, M. Z., Chew, C. M. & Ismail, A. F. 2021 A review on the use of membrane technology systems in developing countries. *Membranes* **12**(1), 30.

Pashkevich, M. A. & Petrova, T. A. 2019 Recyclability of ore beneficiation wastes at the Lomonosov Deposit. *Journal of Ecological Engineering* **20**(2), 27–33.

Phawachalotorn, C., Wongniramaikul, W., Taweekarn, T., Kleangklao, B., Pisitaro, W., Limsakul, W. & Choodum, A. 2023 Continuous phosphate removal and recovery using a calcium silicate hydrate composite monolithic cryogel column. *Polymers* **15**(3), 539.

Possenti, E., Colombo, C., Realini, M., Song, C. L. & Kazarian, S. G. 2021 Time-resolved ATR–FTIR spectroscopy and macro ATR–FTIR spectroscopic imaging of inorganic treatments for stone conservation. *Analytical Chemistry* **93**(44), 14635–14642.

Preisner, M. & Smol, M. 2022 Investigating phosphorus loads removed by chemical and biological methods in municipal wastewater treatment plants in Poland. *Journal of Environmental Management* **322**, 116058.

Revellame, E. D., Fortela, D. L., Sharp, W., Hernandez, R. & Zappi, M. E. 2020 Adsorption kinetic modeling using pseudo-first order and pseudo-second order rate laws: A review. *Cleaner Engineering and Technology* **1**, 100032.

Sambuu, M. 2021 Solubility property of Baganuur coal: Performance assessment by FTIR spectroscopic analysis. *Solid State Phenomena* **323**, 28–41.

Zhao, D., Qiu, S. K., Li, M. M., Luo, Y., Zhang, L. S., Feng, M. H. & Wang, F. 2022 Modified biochar improves the storage capacity and adsorption affinity of organic phosphorus in soil. *Environmental Research* **205**, 112455.

First received 12 September 2023; accepted in revised form 27 October 2023. Available online 10 November 2023